Explicit wavefield extrapolation directly from topography

Saleh M. Al-Saleh, Gary F. Margrave, and John C. Bancroft, University of Calgary*

Summary

Downward continuation methods assume that extrapolation takes place between two planes, but most land surveys are acquired over irregular surfaces. Most approaches that allow downward continuation methods to handle such data, like the wave equation datuming and zero-velocity layer methods, require some processing prior to migration. In this paper, we show how explicit wavefield extrapolation methods in the space-frequency domain can efficiently extrapolate data directly from rugged topography. By building operators with different depth steps, these wavefield extrapolators can handle lateral velocity and topographic variations. We use a source-receiver migration technique to illustrate how this approach can be implemented, using a synthetic dataset as an example.

Introduction

Space-frequency wavefield extrapolation methods are powerful in handling complicated subsurface structures, but unlike ray-based methods, they cannot downward continue directly from irregular surfaces. Further, time shifting the surface recorded data to a flat datum followed by migration is inaccurate for nonvertically traveling energy and can produce artifacts in the shallow section after migration (Gray, 1997). Bevc (1997) used a more accurate approach by upward continuing the data to the highest elevation using wave-equation datuming prior to migration (Berryhill, 1979). However, this can be computationally expensive. The zero-velocity layer approach is more efficient than wave-equation datuming (Beasley and Lynn, 1992; Gray, 1997). In this approach, the data are static-shifted to a horizontal datum above the highest point of the topography prior to migration. Then wavefield extrapolation is carried out by assuming a zero velocity (for diffraction effects only) between the datum and the topography, and the same velocity that is used to calculate the static shifts is used in the thin-lens term. This approach is less expensive than wave equation datuming, but still adds more data to extrapolate. Margrave and Yao (2000) used a variable depth step in the nonstationary phase-shift (NSPS) algorithm to downward continue zero-offset data directly from topography.

In this paper, we present an efficient approach to downward continue data directly from topography by designing wavefield extrapolators with different depth steps. We start with the theory of this approach using a source-migration scheme. Then, the result from the 2D prestack depth migration of a synthetic dataset is shown.

Source-receiver migration with a variable depth step

Source-receiver migration is based on the concept of survey sinking (Claerbout, 1985). That is, after extrapolating the data to a new depth level, the extrapolated wavefield is equivalent to the data that would have been recorded if all sources and receivers were placed on that level. This can be expressed in the space-frequency domain as follows:

$$P(x_r, x_s, n\Delta z, \omega) = \left[\left(\prod_{k=1}^{n} L^r{}_{k\Delta z}\right)\left(\prod_{k=1}^{n} L^s{}_{k\Delta z}\right) P_o\right](x_r, x_s, n\Delta z, \omega), \quad (1)$$

where s is an integer source index ranging from 1 to N (number of sources), r is an integer receiver index ranging from 1 to G (number of receivers), x_s is the source coordinate, x_r is the receiver coordinate, n is a positive integer such that $n\Delta z$ gives the maximum depth of interest, and $P_o = P(x_r, x_s, z = 0, \omega)$ is the surface recorded data. The cascade of operators $\prod_{k=1}^{n} L^s{}_{k\Delta z}$ operates on the source axis to downward continue the receivers according to

$$\prod_{k=1}^{n} L^s{}_{k\Delta z} = L^s{}_{n\Delta z} \circ L^s{}_{(n-1)\Delta z} \circ \ldots\ldots\ldots L^s{}_{1\Delta z}, \quad (2)$$

and the cascade of extrapolators $\prod_{k=1}^{n} L^r{}_{k\Delta z}$ operates on the receiver axis to downward continue the sources according to

$$\prod_{k=1}^{n} L^r{}_{k\Delta z} = L^r{}_{n\Delta z} \circ L^r{}_{(n-1)\Delta z} \circ \ldots\ldots\ldots L^r{}_{1\Delta z}, \quad (3)$$

where

$$\left(L^s{}_{\Delta z} P_o\right)(x_r, x_s, \Delta z, \omega) = \frac{1}{2\pi}\int_{\mathbb{R}} P(x_r', x_s, 0, \omega)\Theta_k(x_r' - x_r, x_r)\, dx_r', \quad (4)$$

$$\left(L^r{}_{\Delta z} P_o\right)(x_r, x_s, \Delta z, \omega) = \frac{1}{2\pi}\int_{\mathbb{R}} P(x_r, x_s', 0, \omega)\Theta_k(x_s' - x_s, x_s)\, dx_s', \quad (5)$$

and "$\circ$" denotes operator composition. The kernel, Θ, of equations (4) and (5), can be written as

Downward continuation from topography

$$\Theta(x-x',x) = \begin{cases} \delta(x-x') & \text{for} \quad \gamma(x) < 0 \\ W_k(x-x',k(x),\gamma(x)) & \text{for} \quad 0 < \gamma(x) < \Delta z \\ W_k(x-x',k(x),\Delta z) & \text{for} \quad \gamma(x) \geq \Delta z \end{cases}, \quad (6)$$

where

$$W_k(x-x',k(x),\Delta\tilde{z}) = -\frac{1}{2\pi}\int_{\mathbb{R}} \hat{W}_k(k_x,k(x),\Delta\tilde{z})\exp(ik_x(x-x'))dk_x, \quad (7)$$

$$k(x) = \frac{\omega}{v_k(x)}, \quad (8)$$

$$\hat{W}_k(k_x,k(x),\Delta\tilde{z}) = \exp(ik_z\Delta\tilde{z}), \quad (9)$$

and

$$k_z = \begin{cases} \sqrt{\frac{\omega^2}{V_k(x)^2} - k_x^2}, & \frac{\omega^2}{V_k(x)^2} > k_x^2 \\ i\sqrt{k_x^2 - \frac{\omega^2}{V_k(x)^2}}, & \frac{\omega^2}{V_k(x)^2} \leq k_x^2 \end{cases}. \quad (10)$$

$h(x)$ is the elevation profile, $\gamma(x) = k\Delta z - h(x)$, and x' and x are the traverse coordinates at input and output, respectively, that can be either x_s or x_r depending the axis of extrapolation. k_x is the transverse wavenumber, ω is the temporal frequency, $V_k(x)$ is the space-variant velocity for a depth level k, and $\Delta\tilde{z}$ can be either Δz or $\gamma(x)$ depending on the depth of the extrapolation level. For practical implementations of equations (4) and (5), the infinitely long operator, W, has to be approximated with a stable operator that is compactly supported.

Claerbout (1985) showed how source-receiver migration can be implemented by migrating one frequency at a time. Here it is implemented by sorting the data into a matrix for each frequency. The rows of each matrix represent the receivers and the columns represent the shots (Figure 1). The matrices that correspond to the different frequencies can be migrated together or independently for one depth level. After each extrapolation, the image can be obtained by invoking the zero-offset and zero-time imaging conditions according to

$$R(n\Delta z, x_r = x_s) = -\frac{1}{\pi}\int_0^\infty diag(P(x_r,x_s,n\Delta z,\omega))d\omega. \quad (11)$$

When the extrapolation level is above the surface elevation, or $\gamma < 0$, the convolution with a delta function returns the original wavefield. However, when the elevation of the input wavefield falls between two extrapolation levels, i.e. $0 < \gamma < \Delta z$, then γ is used as the depth step to build the extrapolator. On the other hand, when the difference between the extrapolation depth level and the elevation of the input wavefield is equal to or greater than Δz, i.e. $\gamma \geq \Delta z$, then the operator is built with Δz. Using equations (4) and (5) simultaneously allows source-receiver wavefield extrapolation to be implemented directly from an irregular surface. Once the extrapolation level is well below the lowest elevation, the same depth step can be used to build all extrapolators.

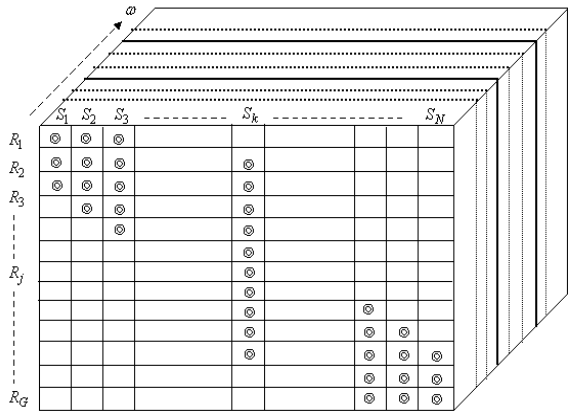

Figure 1: Source-receiver migration can be performed by sorting the data into a matrix for each frequency, where rows represent the receivers and columns represent the shots. N is the number of shots and G is the number of receivers.

Example

The 2D Aruma dataset is used to test this approach. This dataset was generated at Saudi Aramco using a finite difference modeling program. The dataset consists of 626 shots modeled from a rough topography (Figure 2). The maximum number of receivers per shot is 375. The shot and receiver intervals are 16 m. Each shot and receiver was interpolated to 8 m spacing prior to migration. The operators are designed using the FOCI algorithm (Al-Saleh et al., 2006; Margrave et al., 2006) with an operator length of 25 points. Figure 3 shows a shot gather and Figure 4 shows the zero-offset section, where both suffer from the rugged topography. Figure 5a shows the reflectivity model of this dataset (where the arrow indicates the topography), and Figure 5b shows the source-receiver migration result. The deep reflectors are imaged to the right depth and do not suffer from any static distortions. The shallow channels are also well imaged, without any elevation related statics.

Conclusions

Building wavefield extrapolators that can handle not only lateral velocity variations but also topographic changes, allows wavefield extrapolation methods to downward continue data directly from topography. Application of this approach on the Aruma dataset using a source-receiver migration scheme shows that this technique is more efficient than other approaches, such as wave equation datuming and the zero-velocity layer approach, which usually require more steps prior to migration.

References

Al-Saleh S. M., G. F. Margrave, and J. C. Bancroft, 2006, Optimizing the FOCI algorithm with a weighted least-squares approach, 76th Ann. Internat. Mtg., Soc. Expl. Geophys., Expanded Abstracts, this volume.

Beasley, C. J., and W. Lynn, 1992, The zero-velocity layer: migration from irregular surfaces: Geophysics, **57**, 1435–1443.

Berryhill, J. R., 1979, Wave-equation datuming: Geophysics, **44**, 1329–1344.

Bevc, D., 1997, Flooding the topography: Wave-equation datuming of land data with rugged acquisition topography: Geophysics, **62**, 1558–1569.

Claerbout, J. F., 1985, Imaging the earth's interior: Blackwell Scientific Publications, Inc.

Gray, S. H., 1997, Where is the zero-velocity layer?: Geophysics, **62**, 266–269.

Margrave, G. F., and Z. Yao, 2000, Downward continuation from topography with a laterally variable depth step, 70th Ann. Internat. Mtg., Soc. Expl. Geophys., Expanded Abstracts, 481-484.

Margrave, G. F., H. D. Geiger, S. M. Al-Saleh, and M. P. Lamoureux, 2006, Improving explicit depth migration with a stabilizing Wiener filter and spatial resampling: Geophysics, accepted.

Acknowledgements

We thank Sam Gray and Leon Hu for their comments and suggestions. We also wish to thank the sponsors of the CREWES project and the POTSI project, specifically NSERC, MITACS, and PIMS for providing funding and other support. We would also like to thank Saudi Aramco Oil Company.

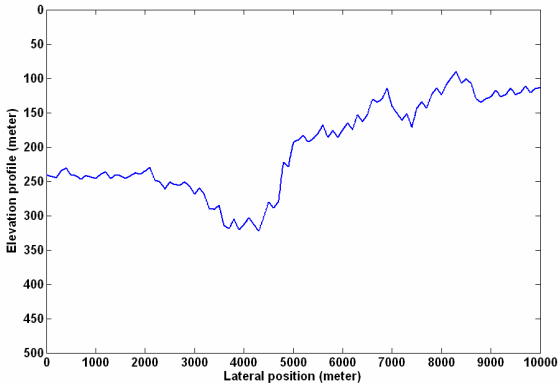

Figure 2: Elevation profile of the Aruma dataset.

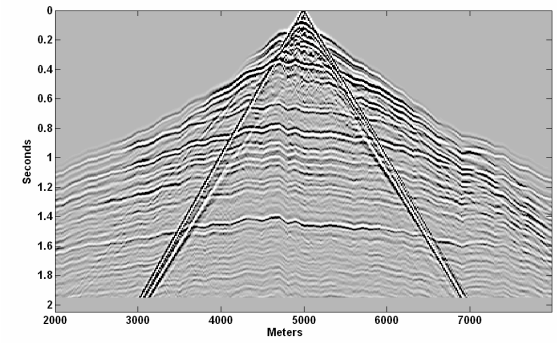

Figure 3: A shot gather from the middle of the line showing the elevation statics problems.

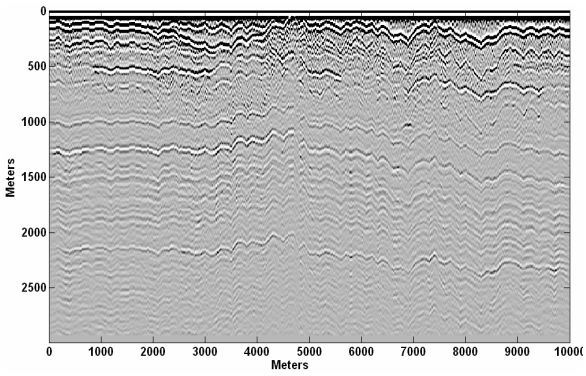

Figure 4: The zero-offset section.

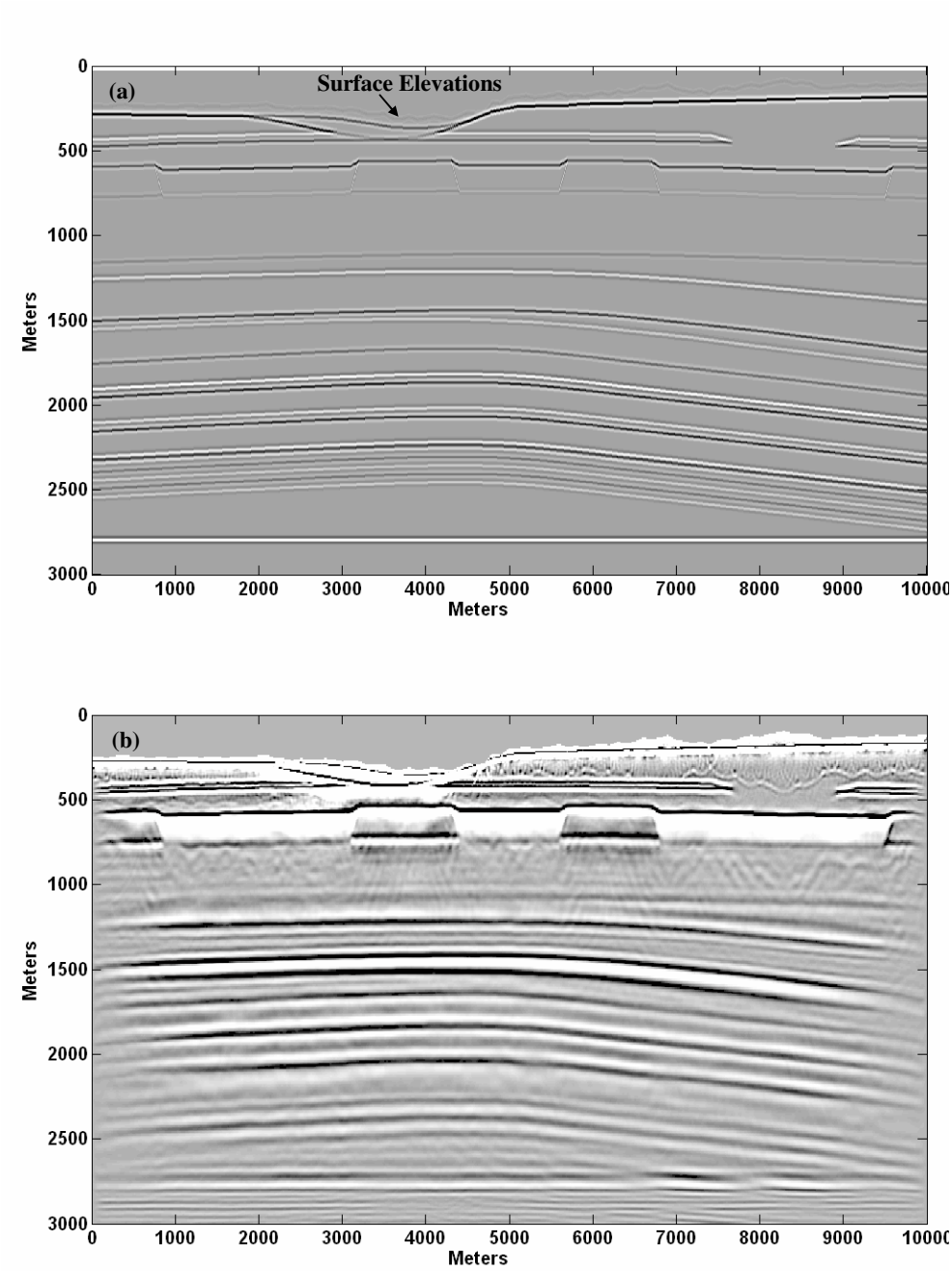

Figure 5: (a) The reflectivity of the Aruma dataset, (b) the source-receiver migration result using the variable depth step approach.